Microbial Biotechnology

WILEY

MICROBIAL BIOTECHNOLOGY Open Access

RESEARCH ARTICLE OPEN ACCESS

The Transcriptional Regulator DhyR Positively Modulates Daptomycin Biosynthesis in *Streptomyces roseosporus*

Fuqiang He[1] | Xinpeng Liu[1] | Haiyi Wang[1] | Xu Li[1] | Yun Wu[2] | Dan Zhang[1] | Shufang Liang[1]

[1]Department of Biotherapy, Cancer Center and State Key Laboratory of Biotherapy, West China Hospital, Sichuan University, Chengdu, Sichuan, P.R. China | [2]Department of Cell Biology, College of Life Science, Sichuan Normal University, Chengdu, Sichuan, P.R. China

Correspondence: Shufang Liang (zizi2006@scu.edu.cn)

Received: 22 November 2024 | **Revised:** 27 January 2025 | **Accepted:** 3 February 2025

Funding: This work was supported by the Basic Research Funding for Colleges and Universities—'From 0 to 1' Innovative Research Program of Sichuan University (2023SCUH0068), and Sichuan Province Science and Technology Support Program (2024ZYD0107).

Keywords: CRISPR-Cas9 | daptomycin | DhyR | *Streptomyces roseosporus* | transcriptional regulator | transcriptome

ABSTRACT

Daptomycin (DAP) is a cyclic lipopeptide antibiotic produced by *Streptomyces roseosporus*, and its biosynthesis is precisely regulated by a complex regulatory network. Although the biosynthetic pathway of DAP has been elucidated, the regulatory mechanism governing its biosynthesis at the transcriptional level is not yet fully understood. In the present study, a new transcriptional regulator, DhyR, was identified. A deletion mutant of *dhyR* was constructed using the CRISPR-Cas9 tool to elucidate the biological role of DhyR thanks to functional and transcriptomic analyses. The results demonstrated that DhyR positively regulates DAP biosynthesis in *S. roseosporus*. The in-frame deletion of the *dhyR* gene resulted in a significant downregulation of the transcription levels of all structural genes within the DAP biosynthetic gene cluster and a significant decrease in DAP yield. In contrast, overexpression of *dhyR* enhanced the transcription levels of the DAP biosynthetic gene cluster, leading to a 23% increase in DAP yield. Deletion of *dhyR* caused significant changes in the expression of multiple genes involved in carbohydrate metabolism, energy metabolism and amino acid metabolic pathways through transcriptome analysis. Especially, deletion of *dhyR* led to a significant downregulation of transcription levels of three DAP biosynthesis-associated genes, including *atrA*, *depR1* and *ssig-05090*. In summary, DhyR positively regulates DAP biosynthesis in *S. roseosporus* by influencing the expression of the DAP gene cluster and modulating precursor flux. It functions as a pleiotropic regulator of primary and secondary metabolism in *S. roseosporus*.

1 | Introduction

Many natural products derived from microorganisms have been developed into drugs to treat various diseases. The genus *Streptomyces*, one of the orders Actinomycetes, is one of the most prolific sources of bioactive natural products. The most remarkable property of *Streptomyces* is that it produces a large number of secondary metabolites with diverse chemical structures, including antibacterial, antitumor, immune suppressant and antiviral compounds (Maksym et al. 2018; Xu and Wright 2019; Lee et al. 2021). Therefore, *Streptomyces* strains, as reservoirs of bioactive natural products, have been widely engineered to discover new natural products or improve yields of target products (Tao et al. 2018).

Daptomycin (DAP) is a cyclic lipopeptide produced by *Streptomyces roseosporus* (*S. roseosporus*), which contains 13 amino acids and a straight-chain decanoic acid attached to the terminal amino group of Trp. Due to its high activity against Gram-positive bacteria, DAP has been approved for the clinical treatment of infections caused by a variety of Gram-positive pathogens, including methicillin-resistant *Staphylococcus aureus* (MRSA), vancomycin-resistant *enterococci* (VRE) and penicillin-resistant *Streptococcus pneumoniae* (Ye et al. 2019;

Zhang et al. 2019). The antibacterial mechanism of DAP is generally thought to be that DAP binds to Ca^{2+} to form a micellar structure in solution and oligomerises in the cell membrane, which results in the dissipation of cell membrane potential and potassium ion efflux, ultimately leading to cell death (Ma et al. 2017; Scott et al. 2007). Because of its clinical importance, several approaches have been employed to improve DAP production, including random mutagenesis with effective high-throughput screening strategies (Yu et al. 2011; Zhou et al. 2023), fermentation process optimisation (Ng et al. 2014), heterologous expression (Choi et al. 2019), metabolic engineering (Huang et al. 2012; Liao et al. 2013; Lyu et al. 2022) and optimisation of the decanoic acid replenishment strategy (Zhu et al. 2023). Although these techniques contribute to DAP titre improvement to a certain extent, there is still a challenge in making a great breakthrough to meet industrial production yield.

The gene cluster for DAP biosynthesis has been clearly elucidated (Miao et al. 2005). The biosynthesis of DAP is initiated by the actions of *dptE* and *dptF*, which are responsible for the activation of fatty acids. The DAP backbone is linearly assembled by three subunits of nonribosomal peptide synthetase (NRPS), including DptA, DptBC and DptD, and then cyclised by the C-terminal thioesterase domain of DptD. The nonproteinogenic amino acid precursors of the DAP backbone include L-3-methylglutamic acid and kynurenine (Kyn), which are formed by the genes *dptI* and *dptJ* (Liao et al. 2013). In addition, the genes *dptP, dptM* and *dptN* are related to DAP resistance or export (Zhang et al. 2021). Three regulatory genes (*dptR1*, *dptR2* and *dptR3*) located adjacent to DAP structural genes were shown to be involved in the regulation of DAP biosynthesis. Some studies report that DptR1 had no effect on DAP production (Zhang et al. 2015; Chen et al., 2022; Ji et al. 2022). However, another study reported that the impact of DptR1 on DAP production is complex and temporarily regulated. The deletion or overexpression of *dptR1* is correlated with an increase and then a decrease in transcriptional levels of the core DAP genes at Day 3 and Day 4, respectively, and resulted in a decrease in DAP production (Yu et al. 2020). DptR2 is required for DAP production but not for the expression of the DAP gene cluster (Wang et al. 2014). DptR3 is a global regulator that positively modulates DAP gene expression and DAP production (Zhang et al. 2015).

The biosynthesis of microbial secondary metabolism is strictly regulated by complex regulatory networks. Several unlinked regulatory loci have been identified using a biotin-labelled *dptE* promoter as a probe in combination with an in vitro affinity purification strategy, including positive regulators AtrA and DepR1, as well as negative regulator DepR2, of DAP biosynthesis (Mao et al. 2015; Yuan et al. 2016; Mao et al. 2017). BldD enhances DAP production by promoting the transcription of the activators DptR3, AdpA and AfsR and of DAP structural genes (Yan et al. 2020). The cyclic AMP receptor protein (Crp), which typically acts as an activator of antibiotic biosynthesis in *Streptomyces*, also enhances DAP production (Wu et al. 2021). The study found that the PhoR-PhoP two-component system responding to phosphate limitation positively regulated DAP production by activating the expression of AtrA. PhoP functions as a positive regulator for DAP biosynthesis by steadily enhancing its own gene expression during phosphate limitation in secondary metabolism (Zheng et al. 2019). Another regulator identified by transposon mutagenesis, PhaR, was also shown to have a negative impact on DAP production (Luo et al. 2018a). WblA, which inhibits the transcription of the positive regulators AtrA and DptR3 and of *dptE*, also has a negative impact on DAP production (Huang et al. 2017). Furthermore, recent studies have shown that DNA methylation and protein crotonylation also play a role in DAP biosynthesis. The deletion of the m4C methyltransferase *sroLm3* significantly enhanced DAP production and resulted in the production of a deep-brown pigment on ISP4 and MM solid medium. Additionally, the metabolic profile of the *sroLm3*-deleted strain was more complex than that of the wild-type (WT) strain, indicating that the promotion of secondary metabolites by in-frame deletion of *sroLm3* was universal in *S. roseosporus* (Fang et al. 2022). Researchers found that the K454 site of DptE undergoes crotonylation, and de-crotonylation of DptE increases initial metabolic flux for DAP biosynthesis (Gao et al. 2024). Therefore, it is very important to identify the genes involved in the regulation of DAP biosynthesis, as this will contribute to the optimisation of DAP biosynthesis and the construction of high-yield DAP strains.

The *dhyR* gene of *S. roseosporus* encodes a predicted protein, DhyR, which possibly belongs to a phenolic acid decarboxylase regulator (PadR)-like transcriptional regulator based on bioinformatics assays. PadR was first reported to be a negative transcription factor for the *padC* gene-encoding phenolic acid decarboxylase. This enzyme converts antimicrobial phenolic acids into less toxic vinyl derivatives (Cheol et al. 2017). PadR homologues are widely distributed in bacteria and are involved in various cellular processes, including virulence, detoxification, antibiotic resistance, antibiotic biosynthesis and carbon catabolism (Sun et al. 2018).

Our previous RNA sequencing of the original WT *S. roseosporus* NRRL 11379 and its UV-derived mutant strain, *S. roseosporus* MT19, indicated that the gene *dhyR* was significantly upregulated in *S. roseosporus* MT19. This finding was confirmed by real-time quantitative PCR (RT-qPCR) verification (Figure S1A). However, the functions of PadR family regulators, including DhyR, have rarely been studied in *Streptomyces* secondary metabolism. Herein, we describe the combination of the generation of mutants by the CRISPR-Cas9 system and their comparative transcriptomic analyses with the original strain to investigate DhyR-mediated biological processes in *S.roseosporus*. This study has shown that DhyR acts as an activator of DAP biosynthesis by indirectly upregulating the expression of the DAP gene cluster.

2 | Results

2.1 | Bioinformatics Analysis of the Regulator DhyR

S. roseosporus MT19 is a mutant strain derived from *S. roseosporus* NRRL 11379 through multi-round UV radiation, and it exhibits a relatively higher titre of DAP compared with the parent strain. Since the mRNA level of the gene *dhyR* (*ssig_00649*) was upregulated by 41-fold in *S. roseosporus* MT19 compared to the

original *S. roseosporus* NRRL 11379 (Figure S1A), we aimed to determine the function of this gene in *S. roseosporus* MT19.

The *dhyR* gene is 609 nucleotides long and encodes a 21.5-kDa protein composed of 202 amino acids. The seven putative α-helices and two putative β-strands of DhyR were identified using I-TASSER (https://seq2fun.dcmb.med.umich.edu//I-TASSER/) (Figure S1B). DhyR contains a conserved winged helix–turn–helix (wHTH) DNA binding motif at its N-terminal region consisting of four α-helices (α1, α2, α3 and α4) and two β-strands (β1 and β2), which is characteristic of the PadR family regulators.

2.2 | Construction of *dhyR* Deletion Strain

In *S. roseosporus* MT19, *dhyR* is colocalized with genes encoding an EamA family transporter, a polyketide cyclase, a DinB family protein and a NADAR family protein (Figure 1A). We used the CRISPR-Cas9 system to delete the *dhyR* gene in *S. roseosporus* MT19, constructing the *dhyR* knockout strain *S. roseosporus* ΔdhyR (Figure 1B) (Cobb et al. 2015). The plasmid PCM2-*dhyR*, containing a sgRNA cassette targeting the *dhyR* gene, was introduced into *S. roseosporus* MT19 by conjugation. The double-strand break caused by the Cas9 protein in *S. roseosporus* MT19 was repaired using the editing template from the pCM2-*dhyR* plasmid through homology-directed repair. The expected mutants were randomly selected and identified by PCR analysis. A distinctive band with a size of 847 bp was amplified from *S. roseosporus* ΔdhyR, and a 1456-bp band was obtained from *S. roseosporus* MT19 as predicted (Figure 1C). The PCR product from exconjugant 1 was subsequently sequenced, and the sequences completely matched the upstream and downstream sequences near *dhyR*. The results suggested that the entire *dhyR* gene was successfully deleted from the genome of *S. roseosporus* MT19 (Figure 1D). Subsequently, the complemented strain ΔdhyR+dhyR was obtained by expression of *dhyR* under the control of its own promoter in *S. roseosporus* ΔdhyR, which was already devoid of the plasmid pCM2-*dhyR*.

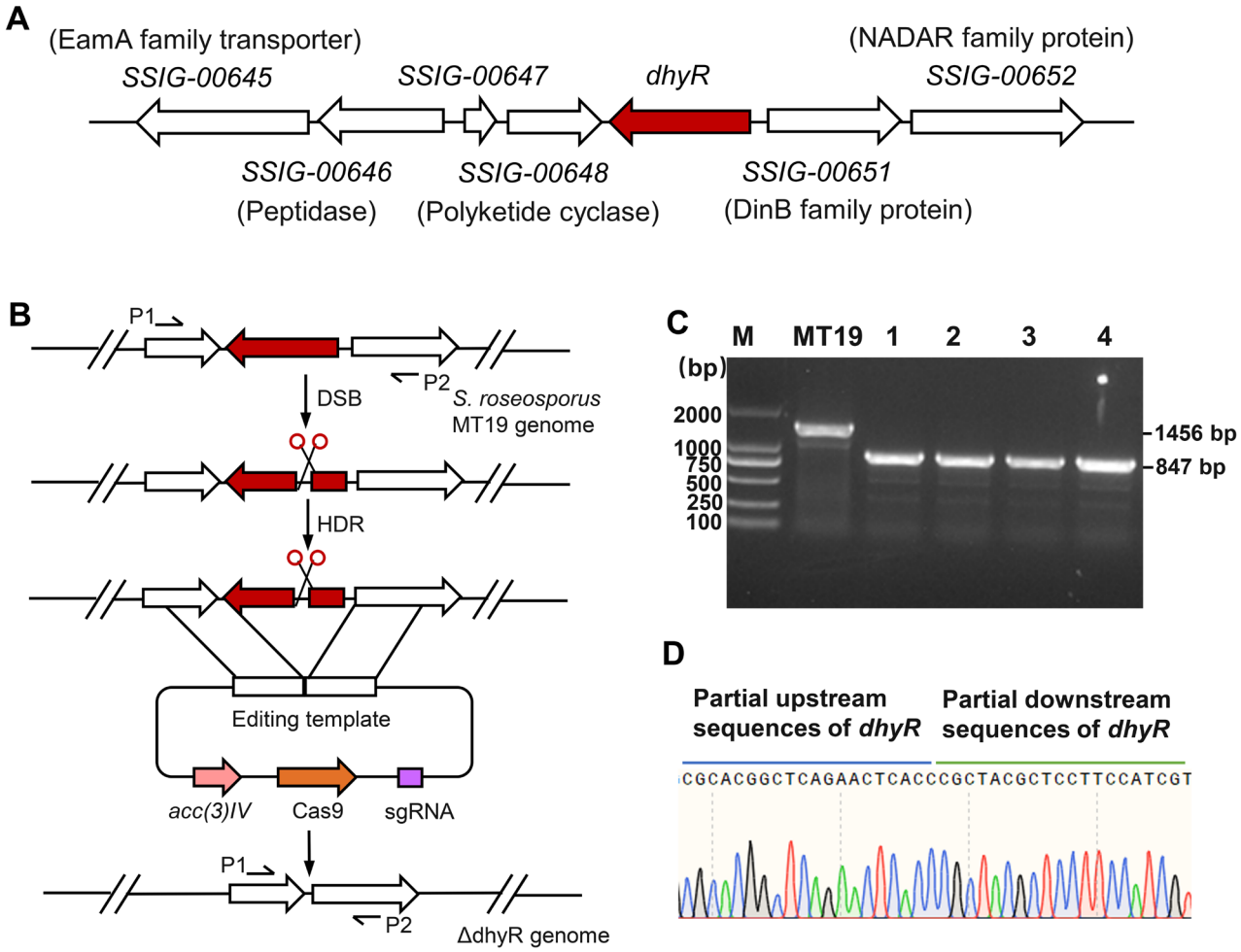

FIGURE 1 | CRISPR-Cas9-mediated *dhyR* gene deletion in *S. roseosporus* MT19. (A) Genetic organisation of *dhyR* and its neighbouring genes. (B) Schematic of CRISPR-Cas9-mediated *dhyR* gene deletion. PCM2-*dhyR*, containing upstream and downstream fragments of *dhyR* and specific sgRNA sequence targeting *dhyR*, was used to delete *dhyR* by CRISPR-Cas9 system. Primers P1 and P2 were used to perform PCR to verify the deletion of *dhyR* gene. Primer P1 locates upstream 385-bp far away from the deletion region. Primer P2 locates downstream 439-bp far away from the deletion region. (C) PCR analysis of *dhyR* gene deletion. Four single colonies (No. 1–4) were randomly chosen to evaluate *dhyR* deletion by PCR with primers P1 and P2. *S. roseosporus* ΔdhyR strain generated 847-bp amplicons, and *S. roseosporus* MT19 strain generated a 1456-bp amplicon. (D) DNA sequencing profiling of the 847-bp PCR fragment amplified from *S. roseosporus* ΔdhyR strain. MT19: *S. roseosporus* MT19; *S. roseosporus* ΔdhyR: *dhyR* deletion strain.

2.3 | Differentially Expressed Genes (DEGs) Between *S. roseosporus* MT19 and *S. roseosporus* ΔdhyR via Transcriptome Analysis

In order to have an insight into the function of DhyR, total RNA was isolated from both *S. roseosporus* MT19 and *S. roseosporus* ΔdhyR strains for RNA sequencing. A total of 16.11 and 16.05 Mb of clean reads were obtained from *S. roseosporus* MT19 and *S. roseosporus* ΔdhyR, respectively. The comparison rates with the reference genome were 99% for *S. roseosporus* MT19 and 98% for *S. roseosporus* ΔdhyR, respectively. For each sample, the coverage of more than 70% of genes was 90%–100% (Figure S2A,B). The number distribution of genes with different expression levels in each sample is shown in Figure S2C. The reads per kilobase million mapped reads (RPKM) value was used to represent gene expression levels. The number of genes with an RPKM value ≥ 100 in *S. roseosporus* ΔdhyR was significantly more than that in *S. roseosporus* MT19.

The DEGs between the two groups typically reflect the biological processes or functions in which *dhyR* is involved. A total of 242 genes showed significant DEGs between *S. roseosporus* MT19 and *S. roseosporus* ΔdhyR. Among the DEGs, 112 genes in the *S. roseosporus* ΔdhyR were significantly upregulated with a fold change of $\geq +2.0$ ($p \leq 0.05$) and 130 genes were significantly downregulated with a fold change of ≤ -2.0 ($p \leq 0.05$) (Figure 2A and Figure S2D).

2.4 | DEGs are Involved in Primary and Secondary Metabolisms of *S. roseosporus* MT19

The Gene Ontology (GO) function enrichment and KEGG pathway analysis of DEGs were performed to further understand *dhyR*-mediated biological functions. According to the GO analysis, DEGs were involved in three aspects of biological categories, including biological processes, cellular components

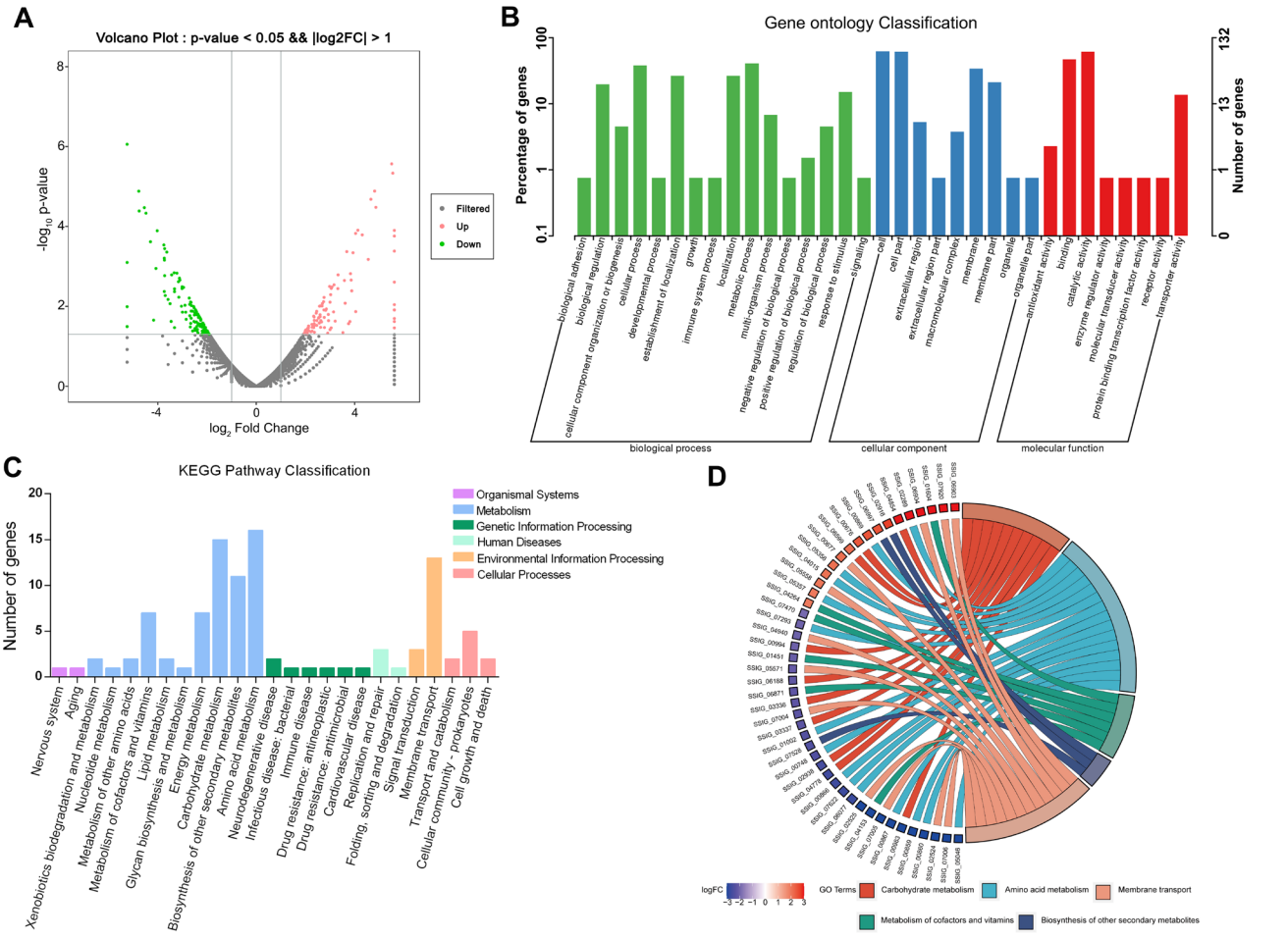

FIGURE 2 | Transcription analysis between *S. roseosporus* MT19 and *S. roseosporus* ΔdhyR strains. (A) Volcano plot of differentially expressed genes between *S. roseosporus* MT19 and *S. roseosporus* ΔdhyR strains. Solid lines represented the applied thresholds (p value < 0.05 and fold change of > +2.0 or < −2.0). The genes presented in green, red or grey indicated the significantly downregulated genes, significantly upregulated genes or the genes with no significant difference, respectively. (B) GO function classification for significantly differentially expressed genes. (C) KEGG pathway classification for significantly differentially expressed genes. (D) The KEGG enrichment plots for significantly differentially expressed genes. On the left side, the gene IDs and their corresponding values of $\log_2$FC were displayed in order from top to bottom. On the top, the values of $\log_2$FC are greater than 2 (red), and a larger $\log_2$FC indicated a greater difference of increased abundance. On the bottom, the values of $\log_2$FC are less than −2 (blue), and a smaller $\log_2$FC means a greater difference of decreased abundance. Five significantly enriched pathways were shown at the bottom of the figure. *S. roseosporus* ΔdhyR: *dhyR* deletion strain.

and molecular functions. In biological process ontology, DEGs involved in biological regulation, cellular process, localisation, metabolic process, regulation of biological process and response to stimulus were significantly enriched. In cell component ontology, DEGs related to cell, cell part, membrane and membrane part were enriched. In molecular function ontology, binding, catalytic activity and transporter activity items had significant differences with the largest number of DEGs (Figure 2B). These results indicated that *dhyR* exerted a fundamental regulatory function and was involved in both primary and secondary metabolisms of *S. roseosporus*.

KEGG pathway analysis enables the identification of major biochemical pathways and signal transduction pathways. DEGs between *S. roseosporus* MT19 and *S. roseosporus* ΔdhyR were mainly enriched in carbohydrate metabolism, amino acid metabolism, energy metabolism, biosynthesis of secondary metabolites, metabolism of cofactors and vitamins, environmental information processing and transport and signal transduction (Figure 2C). According to the KEGG enrichment plots, it was found that carbohydrate metabolism and amino acid metabolism pathways were downregulated in response to *dhyR* deletion (Figure 2D).

2.5 | DhyR Positively Regulates DAP Gene Cluster Expression

In the DAP gene cluster, genes involved in DAP biosynthesis are tightly arranged. Furthermore, the expression of the large operon containing all genes required for DAP synthesis is controlled by the single *dptEp* promoter (Figure 3A). *dhyR* gene deletion had an influence on the DAP gene cluster responsible for DAP biosynthesis. The transcription levels of structural genes of the DAP gene cluster were downregulated in *S. roseosporus* ΔdhyR from the transcriptome data analysis. The

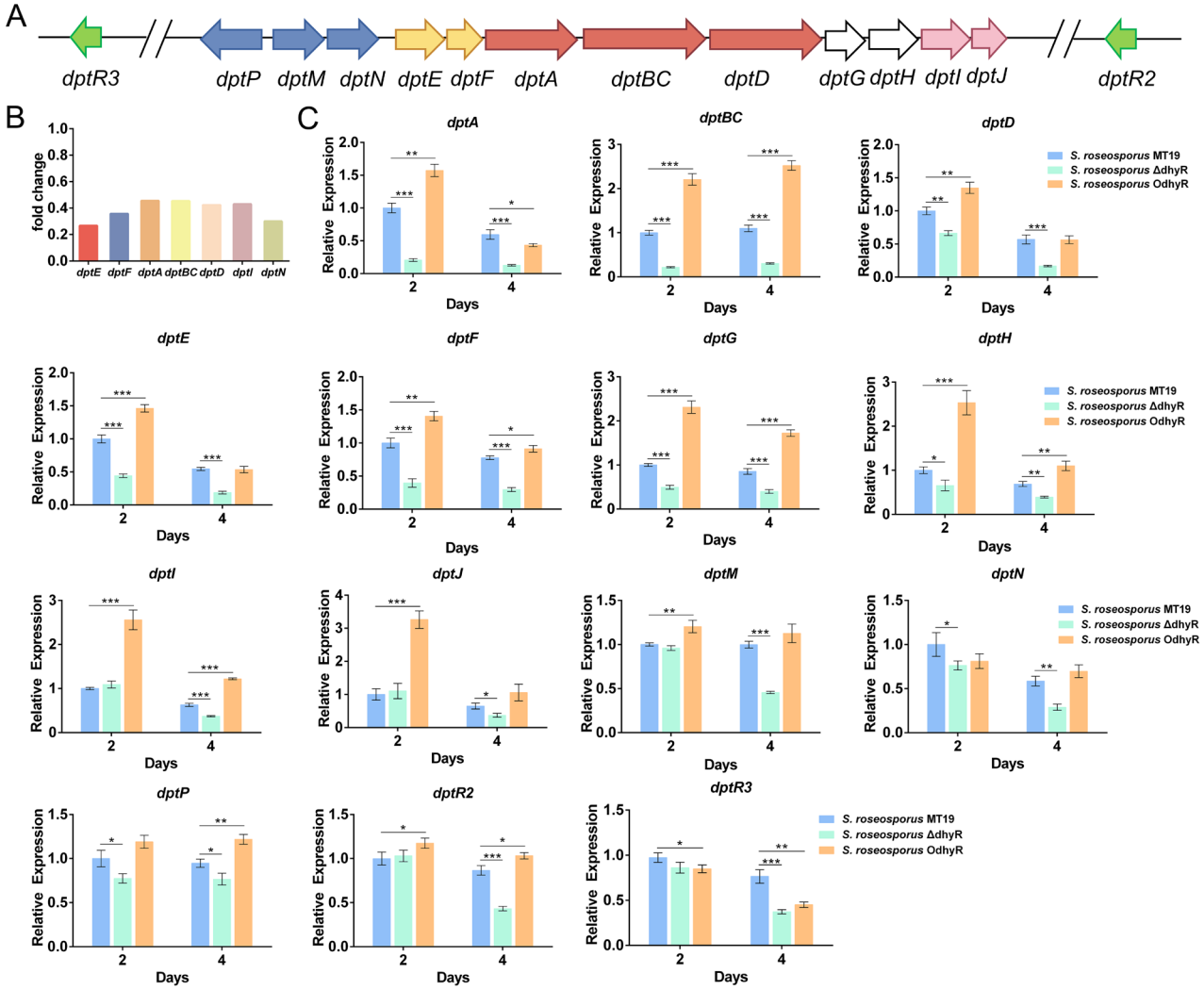

FIGURE 3 | The analysis of the DAP genes transcription levels in the *S. roseosporus* MT19, *S. roseosporus* ΔdhyR and *S. roseosporus* OdhyR strains. (A) The schematic of DAP gene cluster. (B) The relative expression level of DAP genes measured by RNA-seq. (C) RT-qPCR analysis of the DAP genes transcription levels in the *S. roseosporus* MT19, *S. roseosporus* ΔdhyR and *S. roseosporus* OdhyR strains. The relative transcript level of each gene was normalised with that of *S. roseosporus* MT19. The sigma factor gene *hrdB* was used as an internal control. Error bars: Standard deviation for three independent replicates. Statistical significance was determined by Student's *t* test. $*p < 0.05$; $**p < 0.01$; $***p < 0.001$. *S. roseosporus* ΔdhyR: *dhyR* deletion strain, *S. roseosporus* OdhyR: *dhyR* overexpression strain.

transcriptional levels of *dptE* and *dptF* genes were reduced by 3.7-fold and 2.8-fold, respectively. The expression levels of NRPS-encoding genes (*dptA, dptBC* and *dptD*) responsible for DAP skeleton assembly were downregulated by 2.2-fold, 2.1-fold and 2.4-fold, respectively. Moreover, the transcriptional levels of the *dptI* gene and the *dptN* gene were also downregulated by more than 2-fold in *S. roseosporus* ΔdhyR compared to *S. roseosporus* MT19 (Figure 3B). These data indicated that the deletion of *dhyR* had a negative impact on the transcription of DAP structural genes and thus conversely that DhyR had a positive impact on the transcription of these genes. Subsequently, RT-qPCR analysis revealed that the transcription levels of structural genes within the DAP gene cluster, including *dptA*, *dptBC*, *dptD*, *dptE*, *dptF*, *dptG*, *dptH*, *dptI*, *dptJ*, *dptM*, *dptN* and *dptP*, were significantly reduced in *S. roseosporus* ΔdhyR compared to *S. roseosporus* MT19 at exponential phase (2 days of fermentation) or at stationary phase (4 days of fermentation) or at both time points (Figure 3C). These results were consistent with those of our previous transcriptome analysis. Additionally, we assessed the transcription levels of regulatory genes *dptR2* and *dptR3*. The expression levels of *dptR2* and *dptR3* were not affected in *S. roseosporus* ΔdhyR on Day 2 but were significantly downregulated on Day 4 (Figure 3C).

To further evaluate the effect of DhyR on the expression of the DAP gene cluster, we overexpressed the *dhyR* gene in *S. roseosporus* MT19. The resulting strain was named *S. roseosporus* OdhyR. The expression of *dhyR* in this strain was 7.4-fold higher than in *S. roseosporus* MT19 (Figure 4). In *S. roseosporus* OdhyR, the transcription levels of 12 structural genes of the DAP cluster were increased at only one time point or at both time points in response to *dhyR* overexpression (Figure 3C). These results clearly indicated that DhyR positively regulated the expression of the DAP gene cluster.

To assess whether DhyR directly regulates the expression of DAP structural genes, EMSA analysis was carried out using a His6-tagged DhyR recombinant protein and the 5′-biotin-labelled promoter region of *dptE* (*dptEp* probe) (Figure S3A). EMSA results revealed that the purified 6×His-DhyR did not bind to the *dptEp* probe even in the presence of a large amount of protein (2 μg). This indicated that DhyR regulates indirectly the expression of structural genes of the DAP gene cluster (Figure S3B).

2.6 | DhyR Affects DAP Production of *S. roseosporus* but not Morphological Differentiation

The spores of *S. roseosporus* MT19, *S. roseosporus* ΔdhyR and *S. roseosporus* OdhyR were streaked on ISP4 medium to observe morphological differences among the strains. The aerial mycelia and sporulation of *S. roseosporus* ΔdhyR and *S. roseosporus* OdhyR strains on Days 2 and 6 were similar to those of their parental strain, *S. roseosporus* MT19 (Figure 5A). This result indicated that the deletion and overexpression of *dhyR* had no effect on morphological differentiation in *S. roseosporus*.

To directly evaluate the effect of *dhyR* deletion and overexpression on DAP production, the strains *S. roseosporus* MT19, MT19/pSET152K, *S. roseosporus* ΔdhyR, ΔdhyR+dhyR and *S. roseosporus* OdhyR were cultured in fermentation medium to measure DAP yield. After 7 days of cultivation at 30°C, the DAP yield of *S. roseosporus* MT19 strain reached 15.41 mg/L. Compared with *S. roseosporus* MT19 strain, the DAP production

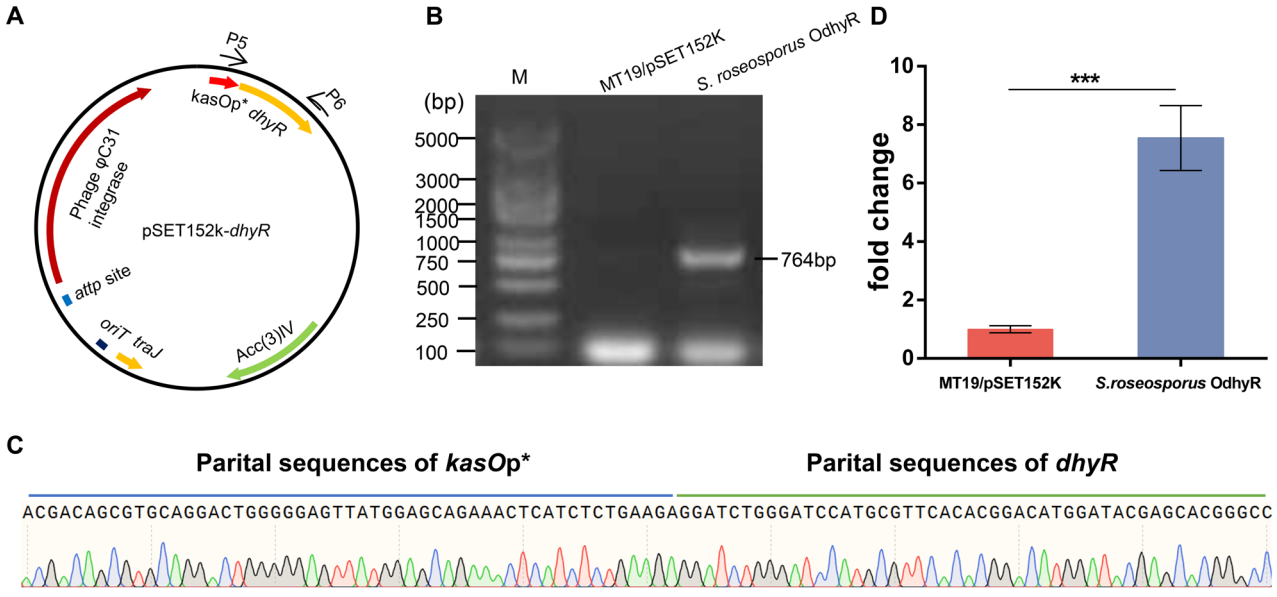

FIGURE 4 | Overexpression of *dhyR* gene in *S. roseosporus*. (A) Schematic overview of pSET152K-*dhyR* plasmid. The *dhyR* gene was driven by the *kasO*p*promoter. (B) The integration of *kasO*p*-*dhyR* cassette into the genome of *S. roseosporus* MT19 by PCR evaluation. The 764-bp *kasO*p*-*dhyR* fragment was amplified from the recombinant genome DNA of *S. roseosporus* MT19 with primers P5 and P6. (C) DNA sequencing profiling of the 764-bp PCR fragment amplified from *S. roseosporus* OdhyR strain. Partial sequences of *kasO*p* and *dhyR* genes were shown in the sequencing map. (D) The analysis of expression level of exogenous *dhyR* gene. The relative transcript level of *dhyR* gene was normalised with that of MT19/pSET152K. The sigma factor gene *hrdB* was used as an internal control. Statistical significance was determined by Student's t test. *$p < 0.05$; **$p < 0.01$; ***$p < 0.001$. MT19/pSET152K: *S. roseosporus* MT19 strain harbouring pSET152K plasmid, *S. roseosporus* OdhyR: *dhyR* overexpression strain.

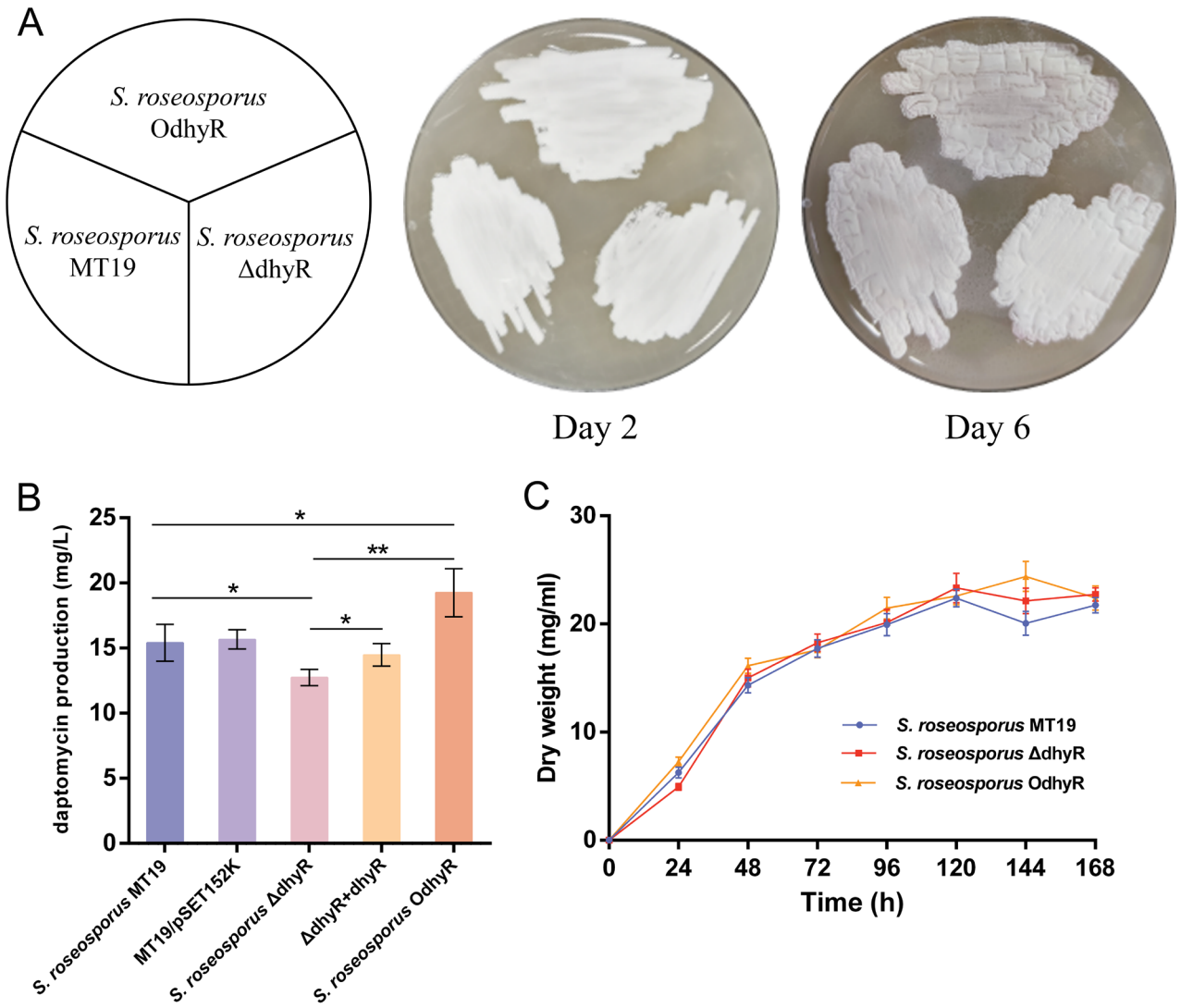

FIGURE 5 | Effects of *dhyR* on phenotype, daptomycin production and cell growth in *S. roseosporus*. (A) Phenotypes of *S. roseosporus* MT19, *S. roseosporus* ΔdhyR and *S. roseosporus* OdhyR strains grown on ISP4 plates at 30°C. (B) Daptomycin production of the *S. roseosporus* MT19, MT19/pSET152K, *S. roseosporus* ΔdhyR, ΔdhyR+dhyR and *S. roseosporus* OdhyR strains. Streptomyces cells were cultured in fermentation medium at 30°C for 7 days. (C) Growth curves of the *S. roseosporus* MT19, *S. roseosporus* ΔdhyR and *S. roseosporus* OdhyR strains cultured in fermentation medium. Cell growth was measured in cell dry weight. Data represent the means ± standard deviations from three independent experiments. MT19/pSET152K: *S. roseosporus* MT19 strain harbouring pSET152K plasmid, *S. roseosporus* ΔdhyR: *dhyR* deletion strain, ΔdhyR+dhyR: *dhyR*-complemented strain, *S. roseosporus* OdhyR: *dhyR* overexpression strain.

of *S. roseosporus* ΔdhyR strain was reduced by 18%, while an approximately 23% enhancement in DAP production was observed in *S. roseosporus* OdhyR strain (Figure 5B). There was no significant difference in the yield of DAP between the control strain MT19/pSET152K and *S. roseosporus* MT19. In addition, the results indicated that the level of DAP in the complemented strain ΔdhyR+dhyR was restored to a similar level as that of *S. roseosporus* MT19 (Figure 5B). These findings indicated that DhyR functions as an activator in DAP production.

The biomass of *S. roseosporus* MT19, ΔdhyR and OdhyR was monitored throughout the fermentation period to determine whether overproduction of DAP was associated with cell growth. The biomass of all strains accumulated rapidly during the first 2 days. Subsequently, the growth of all strains slowed down and entered the stable phase on the 5th day of fermentation. The results showed that there were no significant differences in dry cell weight among all three strains (Figure 5C). These results suggested that DhyR had no influence on cell growth in *S. roseosporus*, and the difference in DAP production between *S. roseosporus* ΔdhyR and *S. roseosporus* OdhyR strains was not caused by changes in cell growth.

2.7 | Deletion of *dhyR* Induces Other Regulatory Genes to Modulate DAP Gene Expression

The results of our EMSA experiments suggest that DhyR did not directly regulate the expression of the DAP gene cluster (Figure S3). Therefore, we speculated that *dhyR* indirectly regulated the expression of the DAP gene cluster via the regulation of the expression of other transcription regulators. We found that AtrA and DepR1, two positive regulators of DAP biosynthesis, were downregulated by 3.5-fold and 1.9-fold in *S. roseosporus*

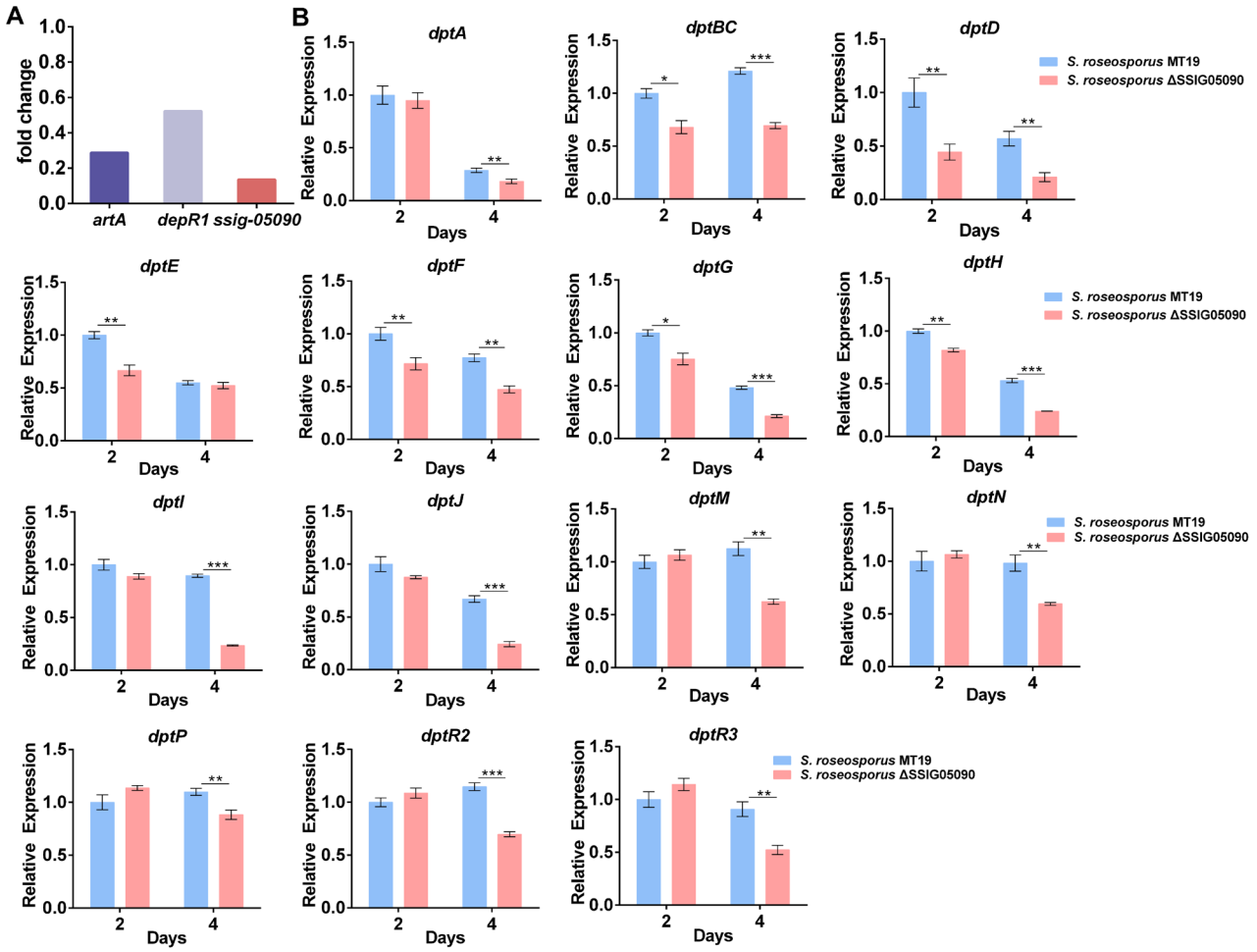

FIGURE 6 | Real-time RT-PCR analysis of the DAP genes transcription levels in the *S. roseosporus* MT19 and *S. roseosporus* ΔSSIG_05090 strains. (A) Relative transcriptional levels of transcriptional regulators related to DAP production. (B) Effect of *ssig_05090* on transcription level of DAP genes. The relative transcript level of each gene was normalised with that of *S. roseosporus* MT19. The sigma factor gene *hrdB* was used as an internal control. Error bars: Standard deviation for three independent replicates. Statistical significance was determined by Student's t test. $*p < 0.05$; $**p < 0.01$; $***p < 0.001$. *S. roseosporus* ΔSSIG_05090: *ssig_05090* deletion strain.

ΔdhyR, respectively (Figure 6A). The lower levels of AtrA and DepR1 might thus be responsible, at least in part, for the decrease in DAP production. However, EMSA results showed that DhyR could not directly interact with *atrA* or *depR1* promoter regions (Figure S3D,E).

In addition, the transcription levels of 11 transcriptional regulators were also significantly changed due to the deletion of *dhyR* (fold change of $> \pm 4.0$, $p \leq 0.05$). We thus constructed knockout mutant strains for each of the 11 transcriptional regulators with the CRISPR-Cas9 system. Since the core genes responsible for DAP biosynthesis are transcribed as a large polycistronic transcript, the expression level of *dptE* was examined by RT-qPCR analysis. Among the 11 transcriptional regulators, deletion of *ssig_05090* (encoding WhiB family transcriptional regulator) significantly reduced the *dptE* expression levels. Furthermore, the expression level of the *ssig_05090* gene was 3.37-fold downregulated in the *S. roseosporus* ΔdhyR and1.6-fold upregulated in the *S. roseosporus* OdhyR compared to the *S. roseosporus* MT19 (Figure 7A). Subsequently, the transcription levels of those genes related to DAP biosynthesis were detected in *S. roseosporus* MT19 and *S. roseosporus* ΔSSIG_05090 strains. As a result, the transcription levels of the genes responsible for DAP synthesis and transport were significantly reduced at least at one time point in *S. roseosporus* ΔSSIG_05090 compared to the *S. roseosporus* MT19 (Figure 6B). The transcription levels of the regulatory genes *dptR2* and *dptR3* were also significantly reduced at 96 h. Furthermore, we demonstrated that the overexpression of *ssig_05090* in the *S. roseosporus* ΔdhyR led to an enhanced expression of the core genes of the DAP gene cluster. The overexpression of this gene thus alleviated the downregulation of DAP gene cluster expression caused by the deletion of *dhyR* in the *S. roseosporus* MT19 strain (Figure 7B). The results indicated that the downregulation of *ssig_05090* might also be one of the reasons for the decreased DAP biosynthesis in the *S. roseosporus* ΔdhyR strain.

2.8 | DhyR Affects DAP Biosynthesis Through Primary Metabolism

Transcriptome data, as well as RT-qPCR experiments (Figure 8A), demonstrated that four genes involved in carbon

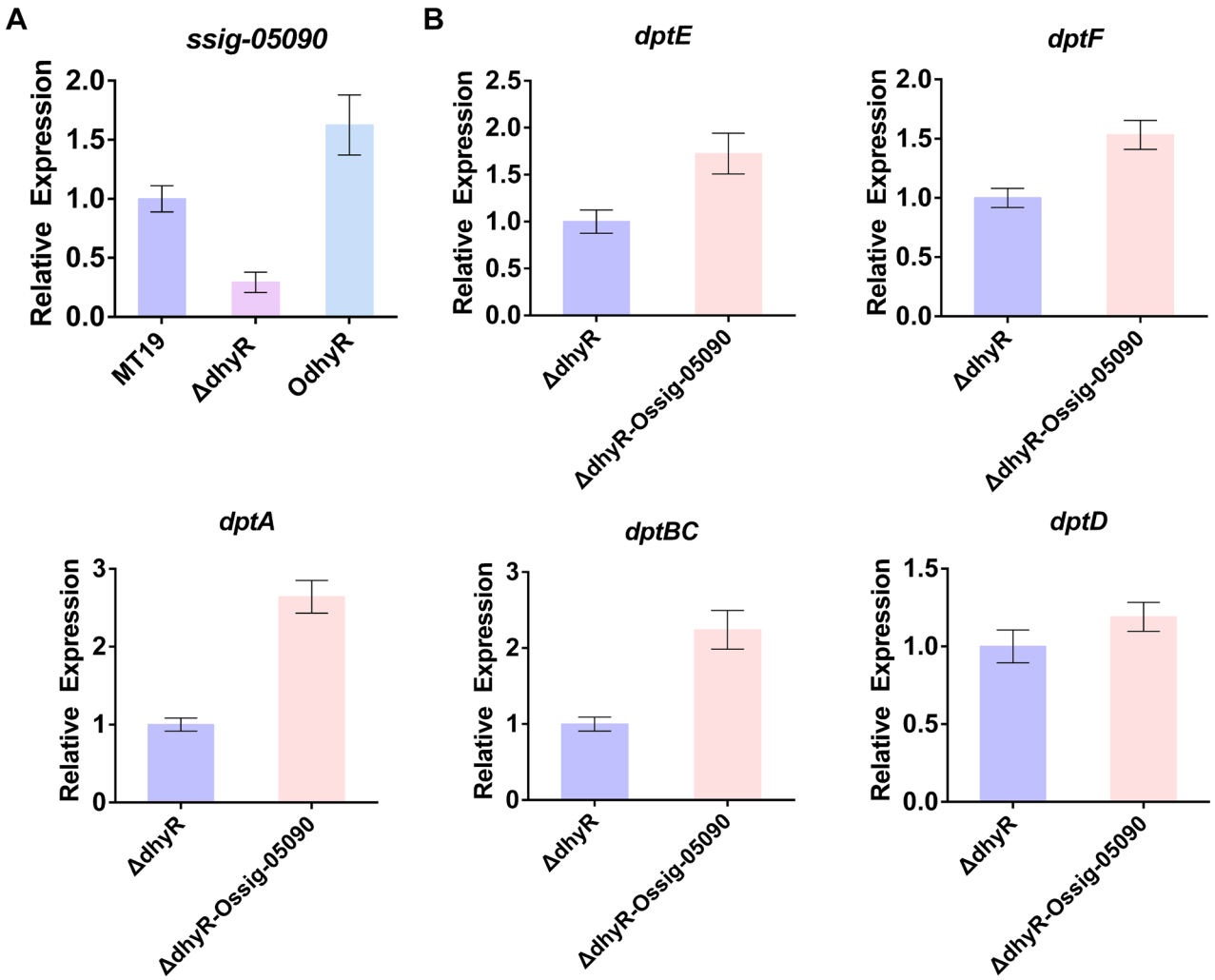

FIGURE 7 | Overexpression of the *ssig_05090* gene improved the expression level of DAP gene cluster in the *S. roseosporus* ΔdhyR strain. (A) Changes in the transcription levels of the *ssig_05090* gene in *S. roseosporus* ΔdhyR and *S. roseosporus* OdhyR. (B) The relative transcript levels of DAP genes in the ΔdhyR-Ossig-05090 strain by RT-qPCR analysis. The relative transcript level of each gene was normalised with that of *S. roseosporus* ΔdhyR. The sigma factor gene *hrdB* was used as an internal control. ΔdhyR-Ossig05090: Overexpression of *ssig_05090* gene in *S. roseosporus* ΔdhyR.

metabolism were significantly downregulated in *S. roseosporus* ΔdhyR, including the gene *ssig_03337* encoding citrate synthase, the gene *ssig_00983* encoding shikimate kinase, the gene *ssig_04778* encoding 2-dehydro-3-deoxygluconokinase (KdgK) and the gene *ssig_05471* encoding propionyl-CoA carboxylase. Citrate synthase is one of the key enzymes in the TCA cycle that provides energy, reducing power and an important precursor for other metabolic pathways. The shikimate kinase catalyses the phosphorylation of shikimic acid to form shikimate-3-phosphate (S3P) that could subsequently be converted into tryptophan, a precursor of DAP biosynthesis. KdgK and propionyl-CoA carboxylase catalyse the formation of 2-keto-3-deoxy-6-phosphogluconate and methylmalonyl-CoA from 2-keto-3-deoxygluconate and propionyl-CoA, respectively, enabling microorganisms to introduce different carbon source metabolic intermediates into the glycolysis pathway and the TCA cycle (Pickl et al. 2014; Liu et al. 2020). In addition, transcriptome data revealed that the expression of glutamate synthase (the gene *ssig_07293*) was also sixfold downregulated in ΔdhyR (Figure 8A). As a central metabolic product, glutamate is involved in the synthesis or results from the degradation of various amino acids, including aspartate, a precursor of DAP.

The five aforementioned genes either alone or with another gene were overexpressed in *S. roseosporus* MT19. These strains were incubated in the fermentation medium to assess their DAP production. The results indicated that the simultaneous overexpression of citrate synthase and shikimate kinase enhanced DAP production by approximately 17%, whereas the overexpression of the other three genes had no impact on DAP biosynthesis (Figure 8B). This result suggested that the citric acid cycle and shikimate pathway might provide energy, reducing power and precursors for DAP biosynthesis.

3 | Discussion

Although the biosynthetic pathway, transcriptional regulation and metabolic engineering related to DAP biosynthesis have been extensively studied, the regulatory mechanism of DAP biosynthesis still remains incompletely understood. In this study,

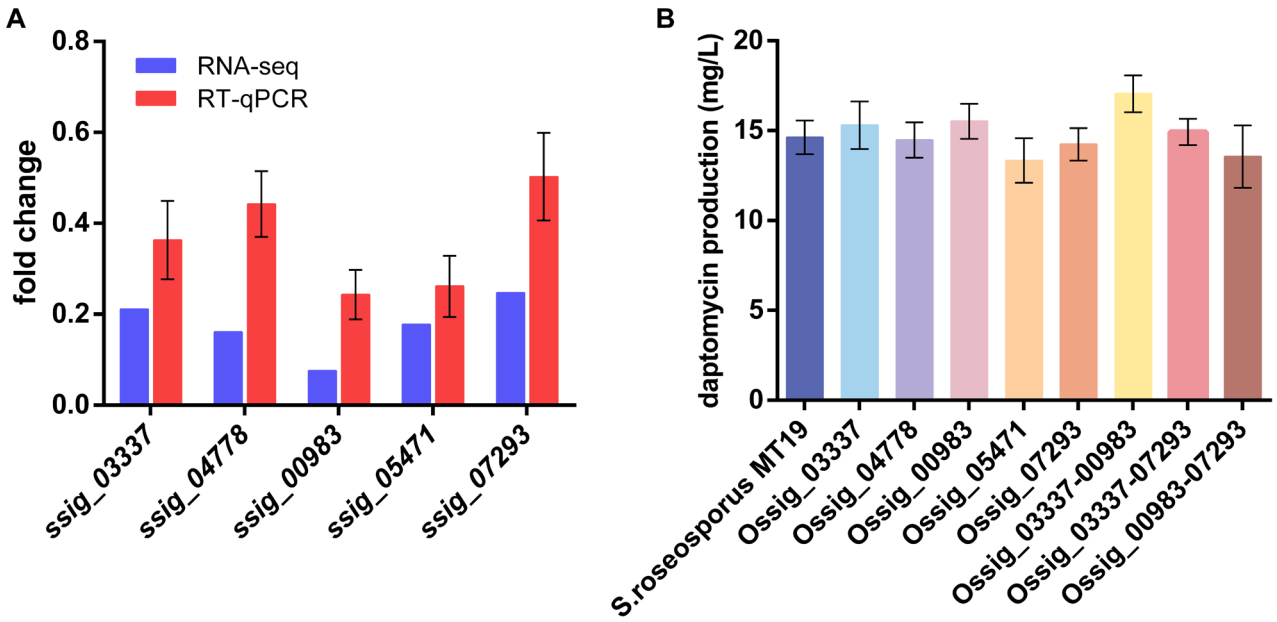

FIGURE 8 | Transcriptional analysis and the effects on DAP production of carbon metabolism genes. (A) The relative expression level of genes measured by RNA-seq and RT-qPCR analysis. The relative transcript level of each gene was normalised with that of *S. roseosporus* MT19. The sigma factor gene *hrdB* was used as an internal control in RT-qPCR analysis. Error bars: Standard deviation for three independent replicates. (B) The yield of DAP of gene overexpression strains. Data represent the means ± standard deviations from three independent experiments. The Ossig-03337, Ossig-04778, Ossig-00983, Ossig-05471 and Ossig-07293 were overexpressed strains of *ssig-03337*, *ssig-04778*, *ssig-00983*, *ssig-05471* and *ssig-07293* genes, respectively. The Ossig-03337-00983, Ossig-03337-07293 and Ossig-00983-07293 were overexpressed strains of two genes, respectively.

using functional genetic experiments with loss (using CRISPR-Cas9) or gain (gene overexpression) of function as well as comparative RT-qPCR and transcriptomic analyses of the original strain with constructed mutant strains, we demonstrated that DhyR plays a role in the regulation of DAP biosynthesis, central metabolism and iron metabolism in *S. roseosporus*.

Indeed, the level of expression of enzymes belonging to different metabolic pathways of central metabolism was either up- or downregulated in the DhyR mutant strain. For instance, the citrate synthase, one of the first enzymes of the TCA cycle that provides energy, reducing power and precursors for other biosynthetic pathways (Huang et al. 2021) was downregulated in the DhyR mutant strain as well as an enzyme of the shikimate pathway that is involved in the supply of tryptophan for DAP biosynthesis. Furthermore, these studies also revealed that DhyR was also involved in iron assimilation and homeostasis (Figure S4) since the deletion of the *dhyR* gene significantly activated the expression of siderophore synthesis and transport pathways in *S. roseosporus*. Our study thus indicated that DhyR can be considered a pleiotropic regulator of primary and secondary metabolism.

DhyR is a PadR-like regulator of unknown function containing a conserved winged wHTH DNA binding domain. PadR family members are broadly distributed in a variety of bacteria and play an important role in virulence, multidrug resistance and detoxification (Lee et al. 2016a), but there are few reports on the function of DhyR and its orthologues in *Streptomyces* species. However, the PadR-like regulators, SrcmRII and MtrY, were shown to be involved in the regulation of antibiotic biosynthesis in some *Streptomyces* species. SrcmRII was shown to negatively regulate chromomycin biosynthesis in *Streptomyces reseiscleroticus* (Cheol et al. 2017) and MtrY was shown to play a dual role in the expression of the mithramycin gene cluster (Ana et al. 2015).

Transcriptome and RT-qPCR analyses supported that DhyR played a positive role in transcript levels of biosynthetic genes for DAP. In general, the transcriptional efficiency of genes in the DAP gene cluster has been suggested to be directly related to DAP production. The expression levels of all structural genes in the DAP gene cluster were significantly upregulated in *S. roseosporus* OdhyR, which may be the main reason for the increase in DAP production. Numerous other strategies were used to increase DAP biosynthesis. The production of DAP was significantly improved by optimising the expression of the DAP gene cluster with promoters of different transcriptional strengths (Ji et al. 2022; He et al. 2024). Furthermore, it was reported that the overexpression of *dptE* and *dptF*, responsible for the activation and acylation of decanoic acid, resulted in a 3.9-fold enhancement of DAP production (Lee et al. 2016b), whereas the introduction of a unique additional copy of *dptJ*, which is responsible for the biosynthesis of Kyn, a necessary precursor for DAP biosynthesis, led to a 110% increase in DAP production (Liao et al. 2013). The *dptP*, *dptM* and *dptN* genes are thought to be involved in the resistance or export of DAP (Zhang et al. 2021). The higher expression of these genes is likely to improve the resistance and export capacity of DAP, and this may be beneficial for DAP overproduction (Ji et al. 2022; He et al. 2024).

However, our negative EMSA results indicated that DhyR was not able to interact with the promoter region of genes of the DAP cluster, suggesting that DhyR may indirectly affect DAP production. This positive effect that DhyR exerts on DAP production might be mediated by the modification of the expression level of other regulators playing a role in the regulation

of DAP biosynthesis. Interestingly, the expression levels of DptR2, DptR3, AtrA and DepR1 were downregulated in the *S. roseosporus* ΔdhyR strain. The regulatory genes *dptR1*, *dptR2* and *dptR3* have been demonstrated to not function as pathway-specific regulators of DAP biosynthesis. The precise functions of DptR1 in regulating DAP production are complex and incompletely understood (Zhang et al. 2015; Chen et al. 2022; Yu et al. 2020). DptR2 has a positive impact on DAP production but is not directly involved in the regulation of the expression of genes of the DAP cluster (Wang et al. 2014). DptR3 enhances DAP production indirectly by altering the transcription of DAP structural genes, and it also stimulates aerial mycelium formation and sporulation on solid media (Zhang et al. 2015). The positive transcription regulators AtrA and DepR1 were retained by the biotinylated *dptEp* DNA fragment as a probe. AtrA directly mediates the A-factor signalling pathway to positively regulate DAP production. AtrA autoregulates its own synthesis and is directly and positively regulated by AdpA and by the phosphate starvation-responsive regulator PhoP (Mao et al. 2015). DepR1 positively regulates DAP production, and the deletion of *depR1* leads to the cessation of DAP production (Yuan et al. 2016). Furthermore, we demonstrated in this issue that the gene *ssig-05090*, which is downregulated in the strain deleted for the *dhyR* gene, also played a positive role in the regulation of DAP gene expression.

In general, the function of DhyR, a PadR-like protein, was systematically described in *S. roseosporus* based on transcriptome and experimental data. We propose that the positive role of DhyR in the expression of DAP biosynthetic genes is likely to be mediated by the control it exerts on the level of expression of positive regulatory genes *atrA*, *depR1*, *dptR2*, *dptR3* and *ssig-05090*, as well as on genes of the central metabolism. Therefore, DhyR functions as a pleiotropic regulator of primary and secondary metabolism in *S. roseosporus*.

4 | Materials and Methods

4.1 | *E. coli* and *S. roseosporus* Strains

S. roseosporus NRRL 11379 was obtained from the American Type Culture Collection (ATCC) (Zhang et al. 2021). The other strains used in this study are listed in Table S1. *E. coli* DH10B was used as a host strain for plasmid construction. *E. coli* ET12567/pUZ8002 was used for conjugation from *E. coli* ET12567 into *Streptomyces* strains.

The homemade mutant strain, *S. roseosporus* MT19, was isolated from the WT strain *S. roseosporus* NRRL 11379 after multiple rounds of UV radiation and antibacterial activity screening experiments. *S. roseosporus* MT19 exhibited an overall enhancement in the metabolite levels and a detectable titre of DAP.

4.2 | Gene Deletion of *dhyR* and *ssig_05090* by CRISPR-Cas9

Plasmids and primers used in this work were listed in Tables S2 and S3. The *dhyR*-deletion and *ssig_05090-deletion* plasmids were constructed using the pCRISPomyces-2 (pCM2) system as previously described (Cobb et al. 2015). The protospacers of *dhyR*-deletion and *ssig_05090*-deletion plasmids were, respectively, designed as 5'-CTTGCGCGCGTCATTGATGA-3′ and 5'-CAGGACCGGTGTTGCCGATG-3′, which corresponded to the last 12-nt sequences plus 3-nt PAM sequences (15-nt total) to meet their specificities. The protospacers were synthesised and inserted into the pCM2 plasmid by golden gate, respectively. Then, two fragments flanking *dhyR*, functioning as the repair template containing 1531-bp upstream and 1476-bp downstream sequences, were amplified from genomic DNA. Similarly, two fragments flanking *ssig_05090* with 1508-bp upstream and 1519-bp downstream sequences were also amplified from genomic DNA. The two pairs of fragments were ligated into the XbaI-digested pCM2 plasmid containing the spacer to generate the *dhyR* deletion plasmid pCM2-*dhyR* and the *ssig_05090* deletion vector pCM2-*ssig_05090* using a one-step cloning kit (C114; Vazyme, Nanjing, Jiangsu, China). The gene-deletion step of *dhyR* and *ssig_05090* was summarised in Figure S5A.

4.3 | Construction of Gene Deletion Strains

The deletion of *dhyR* and *ssig_05090* genes was performed by the CRISPR-Cas9 system. The plasmids pCM2-*dhyR* and pCM2-*ssig_05090* were transferred from *E. coli* ET12567/pUZ8002 to *S. roseosporus* MT19 by conjugation on M-ISP4 solid medium (1 g/L yeast extract, 2 g/L tryptone, 5 g/L soluble starch, 5 g/L D-mannitol, 5 g/L soyal flour, 1 g/L NaCl, 0.1% salt mix, 2 g/L $(NH_4)_2SO_4$, 1 g/L K_2HPO_3, 2 g/L $CaCO_3$, 20 g/L agar and 25 mM $MgCl_2$), respectively. Double-crossover recombinant strains were selected by PCR amplification and sequencing. The correct recombinant strains were transferred to MS solid medium (20 g/L soya flour, 20 g/L D-mannitol and 20 g/L agar) containing apramycin and nalidixic acid for sporulation.

Spores of the correct recombinant strains were collected and transferred to liquid MYG medium (10 g/L malt extract, 4 g/L yeast extract and 4 g/L glucose) without apramycin and nalidixic acid. Since the plasmid pCM2 cannot replicate in *Streptomyces* at 37°C, the MYG medium inoculating spores was incubated initially at 30°C for 24 h and then at 37°C for 48 h to eliminate plasmid pCM2 from *Streptomyces* MT19. Subsequently, the cultures were diluted with MYG medium and then coated on MS solid medium at 30°C for 5 days. Finally, resulting colonies were simultaneously plated on MS and MS solid medium containing apramycin at 30°C to obtain the *dhyR* knockout mutant strain (*S. roseosporus* ΔdhyR) and *ssig_05090* knockout mutant strain (*S. roseosporus* ΔSSIG_05090) without pCM2-*dhyR* and pCM2-*ssig_05090* plasmids.

4.4 | Construction of Overexpression and Complementation Plasmids and Strains

In order to construct the target genes overexpression plasmid, the gene fragments were amplified from *S. roseosporus* MT19 genomic DNA. The *kasOp** fragment from plasmid pkasOp was amplified and digested with XbaI/BamHI. The *kasOp** promoter

was inserted into XbaI/BamHI-digested pSET152 to obtain the pSET152K plasmid (Bierman et al. 1992; Wang et al. 2013). The *dhyR* gene fragment was inserted into the BamHI site of pSET152K to generate the overexpression plasmid pSET152K-*dhyR* using a one-step cloning kit, in which the target genes were driven by the *kasO*p* promoter (Figure S5B). The fragment containing *dhyR* and the *dhyR* promoter region that was amplified was cloned into linearised pSET152 digested with XbaI/BamHI to get the complementation plasmid pSET152-*dhyRp* + *dhyR*.

The pSET152K-*dhyR* plasmid was introduced into *S. roseosporus* MT19 by conjugation to create the overexpression strain. The pSET152-*dhyRp* + *dhyR* plasmid was introduced into *S. roseosporus* ΔdhyR to obtain the complementation strain.

4.5 | Protein Purification and EMSA

For heterologous expression of DhyR in *E. coli*, a DNA fragment encoding 202 amino acids of the DhyR protein was generated by PCR amplification. The PCR fragment was cloned into BamHI/XhoI-digested pET-28a to generate expression vector pET28a-*dhyR*, which was introduced into *E. coli* BL21(DE3) for protein overexpression. After *E. coli* was grown at 37°C to OD600 = 0.6, 0.5 mM IPTG was added to induce the expression of N-terminal His6-tagged DhyR recombinant protein at 16°C overnight. The resulting 6×His-tagged DhyR protein was purified by nickel affinity chromatography according to the manufacturer's instructions (Qiagen). The purified protein was confirmed by SDS-PAGE, and the concentration was determined by the Bradford method.

The 5′-biotin-labelled DNA probes were obtained by high-fidelity PCR from pUC18-*dptEp*, pUC18-*dptR3p*, pUC18-*dptR2p*, pUC18-*dptMp*, pUC18-*atrAp*, pUC18-*depR1p* and pUC18-*ssig-05090* using a 5′-biotin-labelled primer pair. The probes were gel purified and eluted in ultrapure water. EMSA was performed with 1 ng of probes and an increasing amount of protein using the LightShift Chemiluminescent EMSA Kit (20,148, Thermo).

4.6 | Fermentation and Growth Conditions of *S. roseosporus*

S. roseosporus MT19 and mutants were grown in the solid MS medium at 30°C for 5 days to collect spores for fermentation. 1×10^7 spores were added to 250 mL flasks containing 50 mL of MYG liquid medium and incubated at 220 rpm at 30°C for about 36 h. Then the above seed culture was inoculated with a 5% inoculation volume into 200 mL of fermentation medium (0.144 g/L KH_2PO_4, 9 g/L NaCl, 1.06 g/L $Na_2HPO_4 \cdot 12H_2O$, 40 g/L Dextrin, 8 g/L glucose, 10 g/L casein, 2.5 g/L yeast extract and 0.5 g/L $MgSO_4 \cdot 7H_2O$) for fermenting for 7 days at 220 rpm and at 30°C. After 48 h of culture, the feeding medium [the mixture of decanoic acid and methyl oleate (1:1, v/v)] was additionally added to the fermentation medium in the proportion of 5/10,000 every 12 h (Luo et al. 2018b).

In order to detect the growth of *S. roseosporus* MT19 and mutants during fermentation, 5 mL fermentation broth was taken out every 24 h and washed three times with sterile water. The mycelium was dried in an oven at 60°C to determine the dry cell weight.

4.7 | HPLC Analysis of DAP

After fermentation was finished, the pH of the fermentation broth was adjusted to 4.5, and the culture was centrifuged at 6000 rpm for 30 min to extract the supernatant three times with 1/4 volume of n-butanol. The extractions were rotated and evaporated, and the evaporated fermented product was dissolved with chromatographic-grade methanol. One millilitre of fermentation product dissolved in methanol was filtered through a 0.22-mm Millipore membrane.

The target product DAP was analysed by HPLC (1260 Infinity, Agilent) using a C18 reverse-phase column (Zorbax 300SB-C18, 5 μm, 4.6 by 250 mm, Agilent) with Solution A (H_2O containing 0.1% FA) and Solution B (100% acetonitrile) with UV detection set at 214 nm at a flow rate of 1 mL/min. The method set for HPLC was as follows: 0 min, A: B = 75%:25%; 5 min, A: B = 75%:25%; 20 min, A: B = 0%:100%; 40 min, A: B = 0%:100%; 50 min, A: B = 75%:25%; and 55 min, A: B = 75%:25%. Pure DAP was used as a standard.

4.8 | RNA Isolation and RT-qPCR

Total RNA was extracted from mycelia of *S. roseosporus* MT19 and its gene deletion or overexpression mutants were collected in fermentation medium for 48 h and 96 h using TRIzol reagent. One μg total RNA was reverse transcribed into cDNA (HiScript II Q RT Super Mix, R223-01, Vazyme) for real-time RT-PCR analysis (ChamQ SYBR Colour qPCR Master Mix, Q411-02/03, Vazyme) following the previous programme (Zhang et al. 2020). The *hrdB* gene, encoding a sigma factor in *Streptomyces*, was taken as an internal reference to normalise samples. Relative gene expression levels were calculated by the comparative cycle threshold method. Each experiment was performed in triplicate.

4.9 | RNA Sequencing and Data Analysis

Library construction and sequencing of the RNA samples were performed by the OE Biotech Co (Shanghai, China). The rRNA from total RNA of each sample was eliminated using the Rio-off rRNA depletion kit (N407-01, Vazyme) according to the manufacturer's instructions. RNA sequencing library preparation was performed using the TruSeq Stranded mRNA Library Prep Kit (Illumina). Following quality control, the constructed libraries were sequenced on the Illumina Novaseq 6000 platform.

The transcription levels of the genes were analysed, and the threshold to identify DEGs was set at log2(Fold change) ≥ 1 and p value ≤ 0.05. The analysis of the GO annotation and pathway enrichment of DEGs was carried out by the Kyoto Encyclopaedia of Genes and Genomes (KEGG) database.

4.10 | Statistical Analysis

All experiments were carried out in triplicate, and the results were shown as mean ± standard deviation (SD) values. Student's t-test was used to analyse the differences between two groups.

Author Contributions

Fuqiang He: methodology, visualization, writing – review and editing, software, writing – original draft, investigation, formal analysis, validation. **Xinpeng Liu:** validation, investigation, supervision, writing – review and editing. **Haiyi Wang:** investigation, writing – review and editing, validation. **Xu Li:** writing – review and editing, visualization, formal analysis. **Yun Wu:** formal analysis, investigation. **Dan Zhang:** writing – review and editing, conceptualization, formal analysis. **Shufang Liang:** conceptualization, supervision, resources, writing – review and editing, validation, investigation.

Acknowledgements

This work was financially supported by the funds from Sichuan Science & Technology Program (2024ZYD0107) and Basic Research Funding for Colleges and Universities—'From 0 to 1' Innovative Research Program of Sichuan University (2023SCUH0068).

Conflicts of Interest

The authors declare no conflicts of interest.

Data Availability Statement

The data that support the findings of this study are available from the corresponding author upon reasonable request.

References

Ana, B. F., A. L. Susana, Z. Daniel, F. B. Alfredo, A. S. Jose, and M. Carmen. 2015. "Transcriptional Regulation of Mithramycin Biosynthesis in *Streptomyces argillaceus*: Dual Role as Activator and Repressor of the PadR-Like Regulator MtrY." *Microbiology* 161: 272–294.

Bierman, M., R. Logan, K. O'Brien, E. T. Seno, R. N. Rao, and B. E. Schoner. 1992. "Plasmid Cloning Vectors for the Conjugal Transfer of DNA From *Escherichia coli* to *Streptomyces* Spp." *Gene* 116, no. 1: 43–49.

Chen, Q., J. Y. Zhu, X. W. Li, and Y. Wen. 2022. "Transcriptional Regulator DasR Represses Daptomycin Production Through Both Direct and Cascade Mechanisms in *Streptomyces roseosporus*." *Antibiotics* 11, no. 8: 1065.

Cheol, P. S., K. Y. Mi, W. S. Song, M. S. Hong, and S. I. Yoon. 2017. "Structural Basis of Effector and Operator Recognition by the Phenolic Acid-Responsive Transcriptional Regulator PadR." *Nucleic Acids Research* 45, no. 22: 13080–13093.

Choi, S., H. J. Nah, S. Choi, and E. S. Kim. 2019. "Heterologous Expression of Daptomycin Biosynthetic Gene Cluster via *Streptomyces* Artificial Chromosome Vector System." *Journal of Microbiology and Biotechnology* 29, no. 12: 1931–1937.

Cobb, R. E., Y. Wang, and H. Zhao. 2015. "High-Efficiency Multiplex Genome Editing of *Streptomyces* Species Using an Engineered CRISPR/Cas System." *ACS Synthetic Biology* 4, no. 6: 723–728.

Fang, J. L., W. L. Gao, W. F. Xu, et al. 2022. "m4C DNA Methylation Regulates Biosynthesis of Daptomycin in *Streptomyces roseosporus* L30." *Synthetic and Systems Biotechnology* 7, no. 4: 1013–1023.

Gao, W. L., L. Ma, M. H. Li, et al. 2024. "The Faucet Knob Effect of DptE Crotonylation on the Initial Flow of Daptomycin Biosynthesis." *Metabolic Engineering* 87: 1–10.

He, F. Q., X. P. Liu, M. Tang, H. Y. Wang, Y. Wu, and S. Liang. 2024. "CRISETR: An Efficient Technology for Multiplexed Refactoring of Biosynthetic Gene Clusters." *Nucleic Acids Research* 52, no. 18: 11378–11393.

Huang, D., J. Wen, G. Wang, G. Yu, X. Jia, and Y. Chen. 2012. "In Silico Aided Metabolic Engineering of *Streptomyces roseosporus* for Daptomycin Yield Improvement." *Applied Microbiology and Biotechnology* 94, no. 3: 637–649.

Huang, K., B. Zhang, Y. Chen, Z. Q. Liu, and Y. G. Zheng. 2021. "Comparative Transcriptome Analysis of *Streptomyces nodosus* Mutant With a High-Yield Amphotericin B." *Frontiers in Bioengineering and Biotechnology* 8: 621431.

Huang, X., T. Ma, J. Tian, et al. 2017. "*wblA*, a Pleiotropic Regulatory Gene Modulating Morphogenesis and Daptomycin Production in *Streptomyces Roseosporus*." *Journal of Applied Microbiology* 123, no. 3: 669–677.

Ji, C. H., H. Kim, H. W. Je, H. Kwon, D. Lee, and H. S. Kang. 2022. "Top-Down Synthetic Biology Approach for Titer Improvement of Clinically Important Antibiotic Daptomycin in *Streptomyces roseosporus*." *Metabolic Engineering* 69: 40–49.

Lee, C., M. I. Kim, and M. Hong. 2016a. "Structural and Functional Analysis of BF2549, a PadR-Like Transcription Factor From *Bacteroides fragilis*." *Biochemical and Biophysical Research Communications* 483, no. 1: 264–270.

Lee, N., S. Hwang, W. Kim, et al. 2021. "Systems and Synthetic Biology to Elucidate Secondary Metabolite Biosynthetic Gene Clusters Encoded in *Streptomyces* Genomes." *Natural Product Reports* 38, no. 7: 1330–1361.

Lee, S. K., H. R. Kim, Y. Y. Jin, S. H. Yang, and J. W. Suh. 2016b. "Improvement of Daptomycin Production via Increased Resistance to Decanoic Acid in *Streptomyces roseosporus*." *Journal of Bioscience and Bioengineering* 122, no. 4: 427–433.

Liao, G. J., W. Lei, Q. Liu, F. F. Guan, Y. Q. Huang, and C. H. Hu. 2013. "Manipulation of Kynurenine Pathway for Enhanced Daptomycin Production in *Streptomyces roseosporus*." *Biotechnology Progress* 29, no. 4: 847–852.

Liu, X. T., X. J. Feng, Y. M. Ding, et al. 2020. "Characterization and Directed Evolution of Propionyl-CoA Carboxylase and Its Application in Succinate Biosynthetic Pathway With Two CO2 Fixation Reactions." *Metabolic Engineering* 62: 42–50.

Luo, S., X. A. Chen, X. M. Mao, and Y. Q. Li. 2018a. "Transposon-Based Identification of a Negative Regulator for the Antibiotic Hyper-Production in *Streptomyces*." *Applied Microbiology and Biotechnology* 102, no. 15: 6581–6592.

Luo, S., X. A. Chen, X. M. Mao, and Y. Q. Li. 2018b. "Regulatory and Biosynthetic Effects of the *Bkd* Gene Clusters on the Production of Daptomycin and Its Analogs A21978C (1-3)." *Journal of Industrial Microbiology & Biotechnology* 45, no. 4: 271–279.

Lyu, Z. Y., Q. T. Bu, J. L. Fang, et al. 2022. "Improving the Yield and Quality of Daptomycin in *Streptomyces roseosporus* by Multilevel Metabolic Engineering." *Frontiers in Microbiology* 13: 872397.

Ma, W., D. Zhang, G. S. Li, et al. 2017. "Antibacterial Mechanism of Daptomycin Antibiotic Against *Staphylococcus aureus* Based on a Quantitative Bacterial Proteome Analysis." *Journal of Proteomics* 150: 242–251.

Maksym, M., R. Birgit, N. Suvd, P. Petar, N. Philippe, and L. Andriy. 2018. "Generation of a Cluster-Free *Streptomyces albus* Chassis Strains for Improved Heterologous Expression of Secondary Metabolite Clusters." *Metabolic Engineering* 49: 316–324.

Mao, X. M., S. Luo, and Y. Q. Li. 2017. "Negative Regulation of Daptomycin Production by DepR2, an ArsR-Family Transcriptional Factor." *Journal of Industrial Microbiology & Biotechnology* 44, no. 12: 1653–1658.

Mao, X. M., S. Luo, R. C. Zhou, et al. 2015. "Transcriptional Regulation of the Daptomycin Gene Cluster in *Streptomyces roseosporus* by an Autoregulator, AtrA." *Journal of Biological Chemistry* 290, no. 12: 7992–8001.

Miao, V., M. F. Coeffet-LeGal, P. Brian, et al. 2005. "Daptomycin Biosynthesis in *Streptomyces roseosporus*: Cloning and Analysis of the Gene Cluster and Revision of Peptide Stereochemistry." *Microbiology* 151: 1507–1523.

Ng, I. S., C. M. Ye, Z. X. Zhang, Y. H. Lu, and K. J. Jing. 2014. "Daptomycin Antibiotic Production Processes in Fed-Batch Fermentation by *Streptomyces roseosporus* NRRL11379 With Precursor Effect and Medium Optimization." *Bioprocess and Biosystems Engineering* 37, no. 3: 415–423.

Pickl, A., U. Johnsen, R. M. Archer, and P. Schönheit. 2014. "Identification and Characterization of 2-Keto-3-Deoxygluconate Kinase and 2-Keto-3-Deoxygalactonate Kinase in the Haloarchaeon *Haloferax volcanii*." *FEMS Microbiology Letters* 361, no. 1: 76–83.

Scott, W. R., S. B. Baek, D. Jung, R. E. Hancock, and S. K. Straus. 2007. "NMR Structural Studies of the Antibiotic Lipopeptide Daptomycin in DHPC Micelles." *Biochimica et Biophysica Acta-Biomembranes* 1768, no. 12: 3116–3126.

Sun, L., J. Zeng, P. W. Cui, W. Wang, D. Y. Yu, and J. X. Zhang. 2018. "Manipulation of Two Regulatory Genes for Efficient Production of Chromomycins in *Streptomyces reseiscleroticus*." *Journal of Biological Engineering* 12, no. 9: 0103-x.

Tao, W., A. Yang, Z. Deng, and Y. Sun. 2018. "CRISPR/ Cas9-Based Editing of *Streptomyces* for Discovery, Characterization, and Production of Natural Products." *Frontiers in Microbiology* 9: 1660.

Wang, F., N. N. Ren, S. Luo, X. X. Chen, X. M. Mao, and Y. Q. Li. 2014. "DptR2, a DeoR-Type Auto-Regulator, Is Required for Daptomycin Production in *Streptomyces roseosporus*." *Gene* 544, no. 2: 208–215.

Wang, W., X. Li, J. Wang, S. Xiang, X. Feng, and K. Yang. 2013. "An Engineered Strong Promoter for *Streptomycetes*." *Applied and Environmental Microbiology* 79, no. 14: 4484–4492.

Wu, J. Q., D. Q. Chen, J. R. Wu, et al. 2021. "Comparative Transcriptome Analysis Demonstrates the Positive Effect of the Cyclic AMP Receptor Protein Crp on Daptomycin Biosynthesis in *Streptomyces roseosporus*." *Frontiers in Bioengineering and Biotechnology* 9: 618029.

Xu, M., and G. D. Wright. 2019. "Heterologous Expression Facilitated Natural products' Discovery in *Actinomycetes*." *Journal of Industrial Microbiology & Biotechnology* 46, no. 3–4: 415–431.

Yan, H., X. R. Lu, D. Sun, et al. 2020. "BldD, a Master Developmental Repressor, Activates Antibiotic Production in Two *Streptomyces* Species." *Molecular Microbiology* 113, no. 1: 123–142.

Ye, Y., Z. J. Xia, D. Zhang, et al. 2019. "Multifunctional Pharmaceutical Effects of the Antibiotic Daptomycin." *BioMed Research International* 2019: 8609218.

Yu, G., X. Jia, J. Wen, et al. 2011. "Strain Improvement of *Streptomyces roseosporus* for Daptomycin Production by Rational Screening of He-Ne Laser and NTG-Induced Mutants and Kinetic Modeling." *Applied Biochemistry and Biotechnology* 163, no. 6: 729–743.

Yu, G. H., M. Hui, R. F. Li, and S. B. Zhang. 2020. "Pleiotropic Regulation of Daptomycin Synthesis by DptR1, a LuxR Family Transcriptional Regulator." *World Journal of Microbiology and Biotechnology* 36, no. 9: 135.

Yuan, P. H., R. C. Zhou, X. P. Chen, et al. 2016. "DepR1, a TetR Family Transcriptional Regulator, Positively Regulates Daptomycin Production in an Industrial Producer, *Streptomyces roseosporus* SW0702." *Applied and Environmental Microbiology* 82, no. 6: 1898–1905.

Zhang, D., Y. He, Y. Ye, et al. 2019. "Little Antimicrobial Peptides With Big Therapeutic Roles." *Protein and Peptide Letters* 26, no. 8: 564–578.

Zhang, D., X. X. Wang, Y. Ye, et al. 2021. "Label-Free Proteomic Dissection on *dptP*-Deletion Mutant Uncovers *dptP* Involvement in Strain Growth and Daptomycin Tolerance of *Streptomyces roseosporus*." *Microbial Biotechnology* 14, no. 2: 708–725.

Zhang, J., D. Zhang, J. Zhu, H. Liu, S. F. Liang, and Y. Z. Luo. 2020. "Efficient Multiplex Genome Editing in *Streptomyces* via Engineered CRISPR-Cas12a Systems." *Frontiers in Bioengineering and Biotechnology* 8: 726.

Zhang, Q. L., Q. Chen, S. Zhuang, Z. Chen, Y. Wen, and J. L. Li. 2015. "A MarR Family Transcriptional Regulator, DptR3, Activates Daptomycin Biosynthesis and Morphological Differentiation in *Streptomyces roseosporus*." *Applied and Environmental Microbiology* 81, no. 11: 3753–3765.

Zheng, Y., C. F. Sun, Y. Fu, X. A. Chen, Y. Q. Li, and X. M. Mao. 2019. "Dual Regulation Between the Two-Component System PhoRP and AdpA Regulates Antibiotic Production in *Streptomyces*." *Journal of Industrial Microbiology & Biotechnology* 46, no. 5: 725–737.

Zhou, J. Y., B. B. Ma, Q. W. Zhao, and X. M. Mao. 2023. "Development of a Native-Locus Dual Reporter System for the Efficient Screening of the Hyper-Production of Natural Products in *Streptomyces*." *Frontiers in Bioengineering and Biotechnology* 11: 1225849.

Zhu, C. Y., X. Y. Zhao, Z. Y. Lyu, et al. 2023. "Daptomycin Production Enhancement by ARTP Mutagenesis and Fermentation Optimization in *Streptomyces roseosporus*." *Journal of Applied Microbiology* 134, no. 10: 1–10.

Supporting Information

Additional supporting information can be found online in the Supporting Information section.